

## Dust Storms at Al-Ahsa Oasis of Saudi Arabia: A Case Study

Emad A. Almuhanha

Department of Agricultural Systems Engineering, College of agricultural and food sciences, King Faisal University, Al-Ahsa, Saudi Arabia

Received 18 January 2015 - Accepted 10 April 2015

### ABSTRACT

The aim of this study is to characterize dust storm conditions in the arid environment of Al-Ahsa Oasis in Saudi Arabia. Real-time and continuous measurements were done to monitor a severe dust storm struck Al-Ahsa during 12–13 March 2014. This storm caused widespread and heavy dust deposition. A dramatic decrease in visibility with arrival of the storm, and average dust concentrations recorded during a 10-hour peak period were 6,772, 5,862.4 and 451.1  $\mu\text{g}/\text{m}^3$  for total suspended particles (TSP), particle matter smaller than or equal to 10  $\mu\text{m}$  ( $\text{PM}_{10}$ ) and particles smaller than or equal to 2.5  $\mu\text{m}$  ( $\text{PM}_{2.5}$ ), respectively. Particle size distributions show that the geometric mean diameter during the storm was 13.58  $\mu\text{m}$ , based on particle mass concentration. Furthermore, the cumulative percentage of mass concentration for particles of 0.3–25  $\mu\text{m}$  size range shows that the majority were larger than 2.5  $\mu\text{m}$  (> 85%). During the study dust event the quantity of atmospheric dust greatly exceeded air quality limits, which potentially affected human, agricultural, and animal welfare.

**Key words:** Air Quality, Dust storm, Saudi Arabia, Visibility.

### INTRODUCTION

Dust and sand storms and elevated concentrations of particulate matter (PM) are typical problems facing many regions of Saudi Arabia (fig. 1). Sand and dust storms result in hazardous weather and cause major agricultural and environmental problems in many regions of the world.

Regional dust storms negatively affect human life because they carry microorganisms (such as bacteria, fungi, spores, viruses, and pollen) and sharp particles, aggravating asthma, bronchitis, and lung disease (Al-Dabbas *et al.*, 2012). Direct monitoring and theoretical calculation of pollution emissions are the basic methods of atmospheric pollution assessment (Frolova *et al.*, 2007).

The Arabian Peninsula is exposed to outbreaks of consecutive dust storms. A long period of dry weather during the summer months results in greater dryness in the Arabian deserts (Mohalfi, 1995). Dust storms are considered a natural hazard that can affect daily life for periods between several hours to several days (Maghrabi *et al.*, 2011). During certain seasons that account for approximately 30% of the year,

regions of the Middle East such as Saudi Arabia are affected by dust storms. The frequency of dust storm occurrence peaks during the pre-monsoon season (March-May), when dust aerosols are transported by southwesterly winds from arid and semi-arid regions adjacent to the Arabian Sea (Ackerman and Cox, 1989).

According to World Meteorological Organization protocol (Shao and Dong, 2006), dust events are classified by levels of visibility into the following categories:

1. Dust in suspension: widespread dust in suspension in the air that is not raised by wind, either at or near the station at the time of observation; visibility is typically no greater than 10 km
2. Blowing dust: dust or sand raised by wind at the time of observation, reducing visibility to 1–10 km
3. Dust storm: strong winds lift large quantities of dust particles, reducing visibility to between 200 and 1000 m
4. Severe dust storm: very strong winds lift large quantities of dust particles, reducing visibility to less than 200 m.

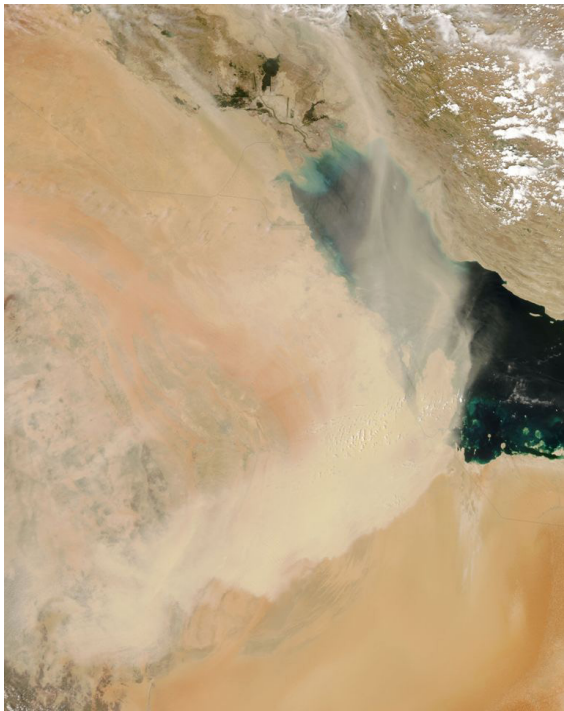


Figure 1: Dust and sand storms in Saudi Arabia, as shown by NASA satellite-based MODIS sensor on 18 April 2008

Most of the dust storm problems are linked to natural factors like variable climate conditions and global warming (increasing aridity and frequency of rainfall which lead to soil erosion), though the connection to man-induced factors, such as land degradation is becoming increasingly evident. A dust storm itself arises from events such as water scarcity, poor biodiversity and desertification. These are all components of a living environment and impart a great impact on human society (Batjargal *et al.*, 2006). The human health impacts of dust storm particulates depend primarily on the mass concentration and the chemical composition of respirable particles, specifically  $PM_{10}$  and  $PM_{2.5}$ . However, the ecosystem health impacts depend mainly on the characteristics of particles deposited on ground surfaces (Gunawardena *et al.*, 2013). Microscopic and toxic particles transported in dust storms can deeply penetrate lungs and other organs, causing severe health problems, e.g., respiratory disorders including asthma, allergies and eye diseases. Moreover, dust particles that penetrate into vegetation pores inhibit plants growth. No

positive effects of dust storms and dustfall have been documented (Chung *et al.*, 2003). Furthermore, particle size is one of the most important parameters for determining the future impact of atmospheric particles. Particle shape and size are critical factors that determine the extent to which particles can penetrate the respiratory tract, the means through which particles are deposited, the location of particle deposition, and the rate of particle clearing from the respiratory tract (Hassan, 2006). Understanding the characteristics of dust will assist development of adequate control measures (Almuhanna *et al.*, 2008, 2009).

Because agricultural and animal production continue to expand rapidly in Saudi Arabia, the facilities where such activities take place and zones surrounding air quality non-attainment areas are faced with major air quality challenges. Wind erosion causes direct damage to crops through plant tissue damage and a reduction in photosynthetic activity, as a result of plant sandblasting, burying of seedlings under sand deposits, and topsoil loss (Fryrear, 1990). Furthermore, dust particles that penetrate vegetation pores inhibit plant growth.

For a long period of time Al-Ahsa oasis of Saudi Arabia has been known by its fertile soil, huge underground water reservoir. However, In recent years the growing phenomenon of drought in addition to dust events have been extraordinary for their intensity and dimensions, furthermore, drifting and settling sand and moving dunes have been devastating the oasis where nearly half of the oasis may have been lost during the past ten centuries (Abdulmalik *et al.*, 2005). Approximately one-third of the Arabian Peninsula is covered by sand dunes. The Jafura sand sea is an elongated sand body 32 by 250 km along the western side of the Arabian Gulf, from Kuwait in the north to the Empty Quarter in the south, a distance of approximately 800 km. The Empty Quarter (Rub' al Khali) likely contains the largest continuous sand dune area in the world, covering nearly 600,000

km<sup>2</sup>. Another 180,000 km<sup>2</sup> is covered by the Great Nafud and Ad Dahna deserts in the interior of the peninsula (fig. 2).

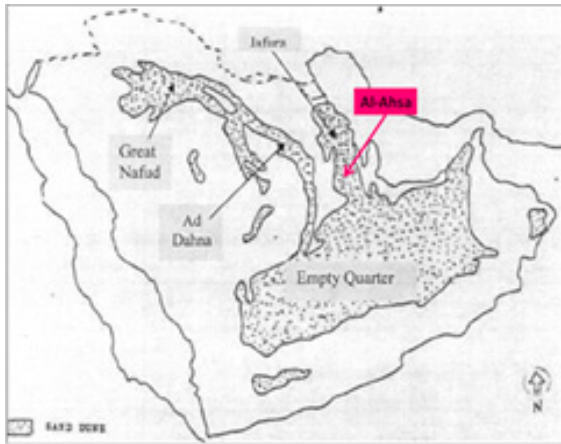


Figure 2: Deserts surrounding Al-Ahsa oasis in Saudi Arabia (Abdulmalik *et al.*, 2005)

Effort were done to study the effects of desertification on Al-Ahsa Oases, Prince Sultan Research Center for Environment, Water and Desert (PSRCEWD) at King Saud University actively participates in local, regional and international studies concerning combating desertification and preservation of ecological balance. It is also a member of the national committee charged with preparing a strategy and concrete plans to combat desertification. One of the prominent projects of the center in the field of combating desertification is “The utilization of remote sensing technologies to study the desertification phenomenon and to confine its spread in Al-Ahsa Oasis project” The project is designed to carry out a scientific study with remote sensing devices to figure out matters such as: the extent of desertification spread in the oasis, the dangerous forms of environment deterioration caused by sand creep, excessive arid conditions, soil erosion due to wind blow, vegetation deterioration, and negative human impacts incurred by more construction of buildings, uprooting palm trees, excessive wood cutting, and over use of pasturelands (PSRCEWD, 2014). Related to this project AL-Saud published some results of this research work entitled “Discrimination of the land features in AL Hasa Oasis, Saudi Arabia, Using Ratio

Technique on Landsat 5 ETM data” (AL-Saud, 2004).

The aim of this study is to describe and to better understand dust storm conditions that might influence human, animal and agriculture in the arid environment of Al-Ahsa oasis. During the study, the following specific goals were achieved: (1) determination of the characteristics of dust events compared with normal conditions; and (2) determination of climatic conditions that interact with dust storms.

## MATERIALS AND METHODS

Sampling and monitoring instruments were installed in the agricultural and veterinary training and research station of King Faisal University (KFU) of Saudi Arabia (25.3°N, 49.6°E, mean altitude above sea level 172 m). This location is ~70 km inland of the seacoast. The following procedures were performed.

1. TSP, PM<sub>10</sub>, PM<sub>2.5</sub> and PM<sub>1</sub> particle levels were continuously recorded using a fixed monitoring station (Turnkey Optical Particle Analysis System, TOPAS), integrated with wind speed and direction sensors with a sampling flow rate 600 cc/min and accuracy ±0.1 µg/m<sup>3</sup>.
2. PM<sub>10</sub> and PM<sub>2.5</sub> continuous measurements were assessed using a filter-based four-stage impactor (model VI-104; HCT Co., Ltd., South Korea) with sampling flow rate 20 l/min, to separate and collect airborne particles in five size ranges of 1.0, 2.5, 5.0 and 10 µm.
3. Airborne particle size distributions (PSD) and number concentrations, real-time numbers and mass concentrations were measured using a particulate matter spectrometer (model PM-101P; HCT Co., Ltd.). This instrument measures particles from 0.3 to 25 µm with air-sampling rate 1 L/min using 15 channels.
4. Particle size distribution data (obtained with the PM-101P, particle counters, VI-104 four-stage impactor) were analysed to determine the distribution type (e.g., lognormal) and mass concentration of

- the various size fractions (TSP, PM<sub>10</sub>, and PM<sub>2.5</sub>).
5. Atmospheric visibility (meteorological optical range) was measured using a Sentry™ SVS1 Visibility Sensor (EnviroTech Sensors, Inc., Columbia, Maryland USA) with visibility range 30–10 km. The sensor uses a light source of 880 nm LED with accuracy ±10% RMSE.
  6. Weather conditions were measured continuously using a HOBO U30 Weather Station (Onset Computer Corp., Bourne, MA, USA) located in the sampling area. Measurements were obtained at four-minute intervals, and average values were recorded at one-hour intervals.

Particle size distributions (number and mass) were analysed by calculating the following statistical variables (Hinds 1999).

Mean diameter:

$$\bar{d}_p = \frac{\sum n_i d_i}{N} \quad (1)$$

Standard deviation (SD):

$$\sigma = \left( \frac{\sum n_i (d_i - \bar{d}_p)^2}{N-1} \right)^{0.5} \quad (2)$$

Geometric mean diameter ( $d_g$  or GMD):

$$d_g = \exp\left(\frac{\sum n_i (\ln d_i)}{N}\right) \quad (3)$$

Geometric standard deviation ( $\sigma_g$  or GSD):

$$\sigma_g = \exp\left(\frac{\sum n_i (\ln d_i - \ln d_g)^2}{N-1}\right)^{0.5} \quad (4)$$

where:

$d_i$  = diameter of particles of size  $i$  ( $\mu\text{m}$ )

$\bar{d}_p$  = mean particle diameter ( $\mu\text{m}$ )

$d_g$  = geometric mean diameter (GMD)

by sample mass ( $\mu\text{m}$ )

$\sigma_g$  = geometric standard deviation (GSD)

$n_i$  = number of particles of size  $i$

$N$  = total number of particles.

Particulate mass concentrations were determined by gravimetric calculation using

$$\text{Conc.} = \frac{W_f - W_i}{Q * t} \quad (5)$$

where:

*Conc.* = concentration ( $\mu\text{g}/\text{m}^3$ )

$W_i$  = filter initial weight ( $\mu\text{g}$ )

$W_f$  = filter final weight ( $\mu\text{g}$ )

$Q$  = sampling system air flow rate ( $\text{m}^3/\text{min}$ )

$t$  = sampling time (min).

Data were statistically analysed using PROC GLM in SAS (version 9.1; SAS Institute, Inc., Cary, NC, USA). Particulate concentration mean comparisons were made using Duncan's multiple range test at significance level 5%.

## RESULTS AND DISCUSSION

On 12 March 2014 at about 10:00 AM, a typically far-reaching and severe dust storm began over Al-Ahsa. This intense storm caused widespread and heavy dust deposition, which greatly affected visibility and air quality (fig. 3).



Figure 3: Strong and sudden dust storm (Al-Ahsa, Saudi Arabia, 12 March 2014), climatic conditions: (a) before storm, (b) during storm

The dust storm originated over northern Saudi Arabia near Kuwait and southern Iraq, moving south toward eastern Saudi Arabia and Al-Ahsa, and then southwest toward the Empty Quarter. Figure 4 shows four images (a, b, c and d) recorded by the Meteosat 0 degree (Dust-Eastern Africa-RGB), which illustrate the development of the dust storm on 12 March.

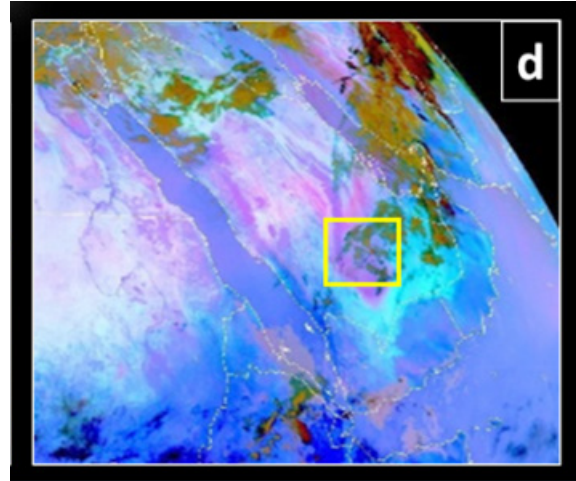
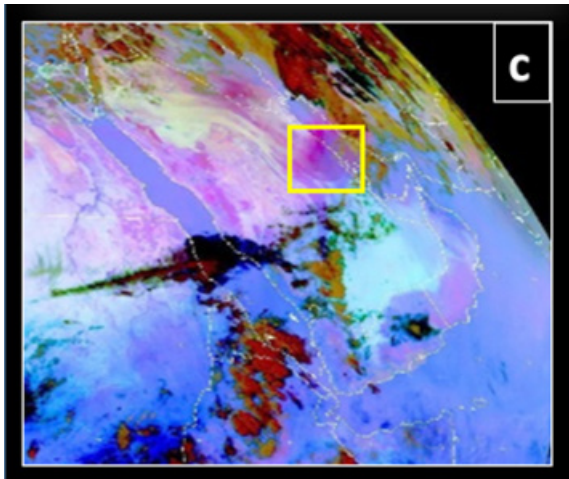
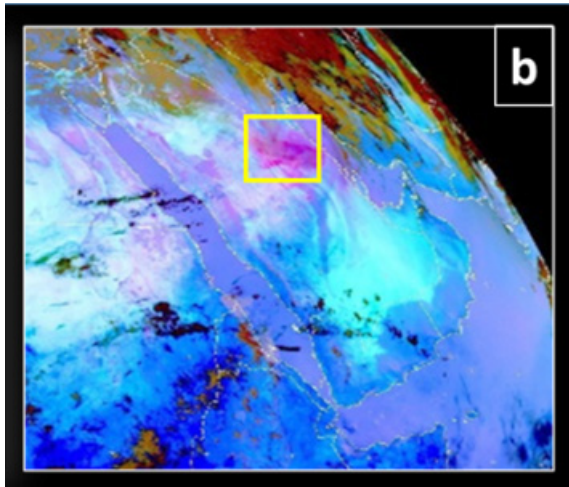
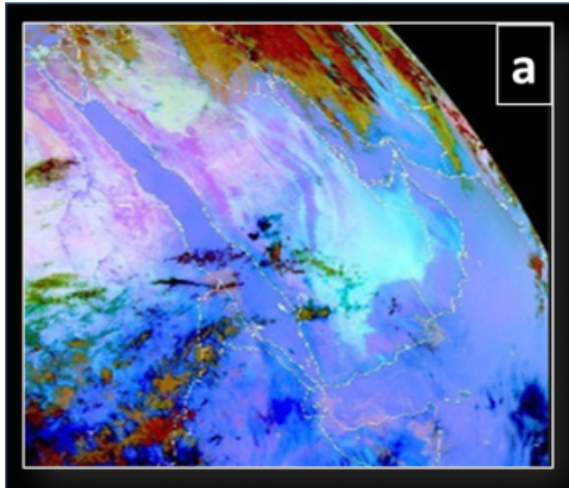


Figure 4: Meteosat 0 degree-Dust-Eastern Africa-RGB images showing dust storm movement on 12–13 March 2014; (a) before storm, (b, c, and d) path of the storm. <Source: <http://oiswww.eumetsat.org/IPPS/html/MSG/RGB/DUST/EASTERNAFRICA/index.htm>, courtesy of EUMETSAT: <http://www.eumetsat.int/website/home/index.html>>. Retrieval Date: 16 March 2014.

### Meteorological conditions associated with dust event

Weather conditions on both the day of the dust storm and days prior were relatively normal. The arrival of the storm accompanied by an air temperature drop of about 9 °C. This resulted in a maximum temperature of 27 °C, compared with the 36 °C average maximum monthly mean temperature (fig. 5). It is likely that this reduction in daytime temperature was produced by reduced surface heating caused by shortwave energy extinction from additional aerosol loads that arrived with the storm. Relative humidity dropped about 10%. This resulted in an average of 29.6%, compared with the 39.9% average monthly mean.

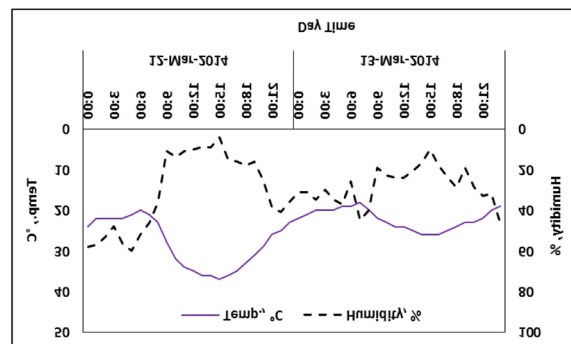


Figure 5: Ambient temperature and relative humidity during dust storm event (12–13 March 2014)

Atmospheric pressure dropped to a minimum of 984.34 mbar (corresponding to 1004 hPa sea level atmospheric pressure) compared with the 993.6 mbar (1014 hPa sea level atmospheric pressure) recorded the day before (fig. 6).

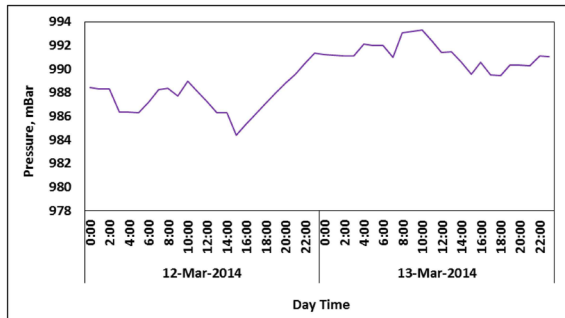


Figure 6: Atmospheric pressure during dust storm (12–13 March 2014)

Furthermore, winds were relatively calm (1.6 m/s) before the dramatic change of wind speed and direction with the arrival of the storm. Wind speeds rapidly increased to a maximum 17.5 m/s. By the end of the day on 12 March, wind speeds dropped again. Before the event began, the wind was from the south (180 degrees). By noon on 12 March with storm initiation, the wind direction shifted to the northwest and then north-northwest, finally settling on northerly by the second day of the event (fig. 7). These trends, illustrated by satellite images, clearly show that the dust storm moved from the north to the northwest part of the Al-Ahsa region. Analysis of the wind data collected at Al-Hofuf (major city in Al-Ahsa) and nearby climatic stations indicates that two semiannual windy seasons occur in Al-Ahsa. The first one occurs from December to January and the second one occurs from April to June. The winds during these seasons are mainly from the northern ( $315^{\circ}$ - $45^{\circ}$ ) directions and therefore, they are locally called shamals (northern winds). They last over 60 days with wind velocities ranging from 5.4 to 15.7 m/sec (Abdulmalik, 2005).

Atmospheric aerosols affect atmospheric visibility by scattering and absorbing shortwave and visible solar radiation. Table 1 and (fig. 8) show dramatic decreases in visibility to 200 m with dust storm arrival. Visibility fluctuated thereafter. By the

evening of 13 March, visibility stabilized at a normal value of 10 km, reflecting conditions similar to those preceding the dust event.

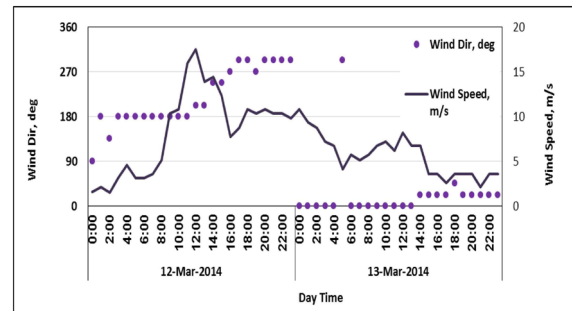


Figure 7: Wind speed and direction during dust storm (12–13 March 2014)

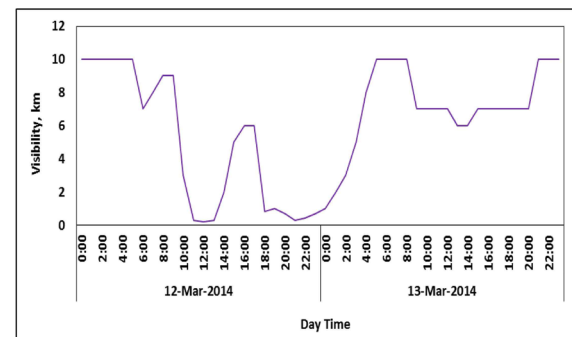


Figure 8: Visibility during dust event on (12–13 March 2014)

### Particle mass concentrations

During the 10-hour dust storm peak, maximum measured PM concentrations were 7389.8, 6500.2 and 491.4  $\mu\text{g}/\text{m}^3$  for TSP,  $\text{PM}_{10}$ , and  $\text{PM}_{2.5}$ , respectively (fig. 9). Ten-hour mean and standard deviation values ( $\mu\text{g}/\text{m}^3$ ) for TSP,  $\text{PM}_{10}$ , and  $\text{PM}_{2.5}$  during peak hours of the dust event are compared with 2013 means in Table 2. These values greatly exceeded threshold limits for both human and animal safety.

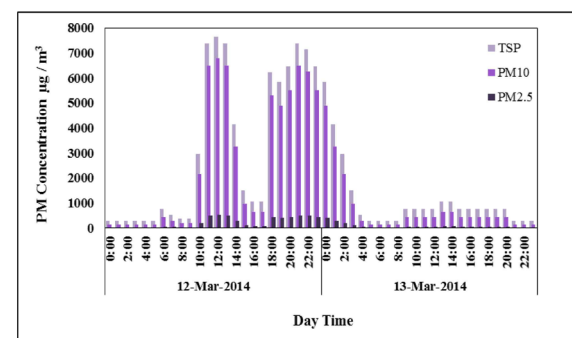


Figure 9: PM concentrations (TSP,  $\text{PM}_{10}$  and  $\text{PM}_{2.5}$ ) during dust event

Table (1): Relationship between weather conditions and visibility values\*

12-Mar-2014			13-Mar-2014		
Time	Visibility, km	Conditions	Time	Visibility, km	Conditions
0:00	10	Scattered Clouds	0:00	1	Widespread Dust
1:00	10	Scattered Clouds	1:00	2	Widespread Dust
2:00	10	Scattered Clouds	2:00	3	Widespread Dust
3:00	10	Scattered Clouds	3:00	5	Widespread Dust
4:00	10	Clear	4:00	8	Scattered Clouds
5:00	10	Clear	5:00	10	Clear
6:00	7	Widespread Dust	6:00	10	Scattered Clouds
7:00	8	Clear	7:00	10	Clear
8:00	9	Unknown	8:00	10	Clear
9:00	9	Blown Sand	9:00	7	Blown Sand
10:00	3	Widespread Dust	10:00	7	Unknown
11:00	0.3	Sandstorm	11:00	7	Unknown
12:00	0.2	Sandstorm	12:00	7	Blown Sand
13:00	0.3	Sandstorm	13:00	6	Unknown
14:00	2	Blown Sand	14:00	6	Unknown
15:00	5	Blown Sand	15:00	7	Widespread Dust
16:00	6	Clear	16:00	7	Clear
17:00	6	Unknown	17:00	7	Clear
18:00	0.8	Widespread Dust	18:00	7	Widespread Dust
19:00	1	Widespread Dust	19:00	7	Clear
20:00	0.7	Widespread Dust	20:00	7	Clear
21:00	0.3	Widespread Dust	21:00	10	Clear
22:00	0.4	Widespread Dust	22:00	10	Clear
23:00	0.7	Widespread Dust	23:00	10	Clear

\*Data source: Weather Underground, Al-Ahsa airport station (OEAH).

Table (2): Ten-hour mean and standard deviation values ( $\mu\text{g}/\text{m}^3$ ) for TSP,  $\text{PM}_{10}$ , and  $\text{PM}_{2.5}$  during dust event, compared with 2013 mean values

Event	TSP		$\text{PM}_{10}$		$\text{PM}_{2.5}$	
	Mean <sup>[*]</sup>	SD	Mean <sup>[*]</sup>	SD	Mean <sup>[*]</sup>	SD
Dust Storm	6772 a	1203.8	5862.4 a	718.7	451.1 a	45.5
2013	783.2 b	547.9	545.6 b	417.5	57.0 b	37.2

\*Column means followed by the same letter are not different at 5% level of significance

Table 3 shows a matrix of relationships between the TSP and  $\text{PM}_{10}$ ,  $\text{PM}_{2.5}$  variables for the dust event and 2013 annual average. These results indicate that most dust particles

propelled during the storm were larger than  $2.5 \mu\text{m}$ . However, this relationship varies based on dust storm type and source plus the timing of dust movement.

Table (3): Matrix of variables showing TSP, PM<sub>10</sub>, and PM<sub>2.5</sub> relationships during dust event, compared with 2013 mean values

	Dust event			2013		
	TSP	PM <sub>10</sub>	PM <sub>2.5</sub>	TSP	PM <sub>10</sub>	PM <sub>2.5</sub>
TSP	1	1.16	15.02	1	1.43	13.74
PM <sub>10</sub>	0.87	1	12.99	0.69	1	9.59
PM <sub>2.5</sub>	0.07	0.15	1	0.07	0.10	1

**Particle size distribution (PSD)**

Particle size is one of the most important parameters determining the effects of atmospheric particles. Although this size is a very important physical property that governs particle behaviour, few investigations of PSD during dust storms have been reported in the literature, and even fewer focus on Saudi Arabia. In this study, the size distribution, number, and mass concentration of airborne particles during a dust storm event occurred during 12-13 March 2014 were monitored. The results are summarized in Table 4.

Table (4): Particle number and mass distributions

Parameter	Number Distribution	Mass Distribution
Mean Diameter (µm)	0.70	16.52
Standard Deviation	1.05	17.71
Geometric Mean Diameter (µm)	0.48	13.58
Geometric Standard Deviation	2.37	18.56

The geometric mean diameter (GMD) based on the numerical distribution was 0.48 µm, and the geometric standard deviation (GSD) was 2.37. Based on the mass distribution, GMD was 13.58 µm and GSD was 18.56. Figure 10 shows PSDs based on number and mass concentrations.

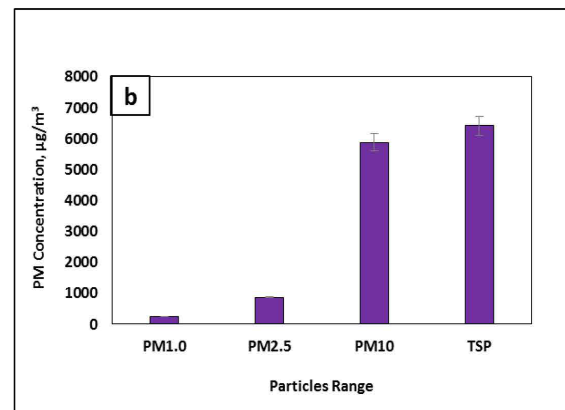
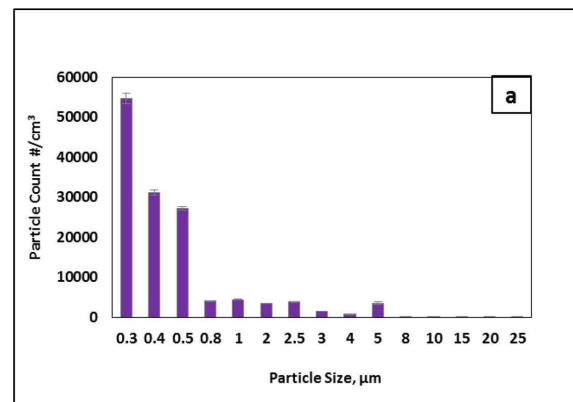


Figure 10: Particle size distributions based on particle (a) number (count) and (b) mass concentrations. Error bars denote standard deviations

The geometric mean diameter (GMD) based on the numerical distribution was 0.48 µm, and the geometric standard deviation (GSD) was 2.37. Based on the mass distribution, GMD was 13.58 µm and GSD was 18.56. Figure 10 shows PSDs based on number and mass concentrations.

Cumulative percentage results of particle based on number concentrations for size range 0.3–25 µm (fig. 11a) show that the majority of particles were smaller than 2.5

$\mu\text{m}$  ( $> 90\%$ ). Cumulative percentages of particle based on mass concentration for size range  $0.3\text{--}25\ \mu\text{m}$  (fig. 11b), demonstrating that a large proportion of particles were larger than  $2.5\ \mu\text{m}$  in diameter ( $> 85\%$ ). This indicates that a significant proportion of dust mass was likely to be deposited in the nasal and pharyngeal regions if inhaled. Over time, the larger particles settled to the surface, leaving the smaller particles suspended in air. This resulted in a smaller GMD and lower concentrations. However, the remaining particles are more dangerous, owing to their ability to penetrate respiratory systems. Settling dust solubility rates and colour characteristics will be discussed in a separate paper.

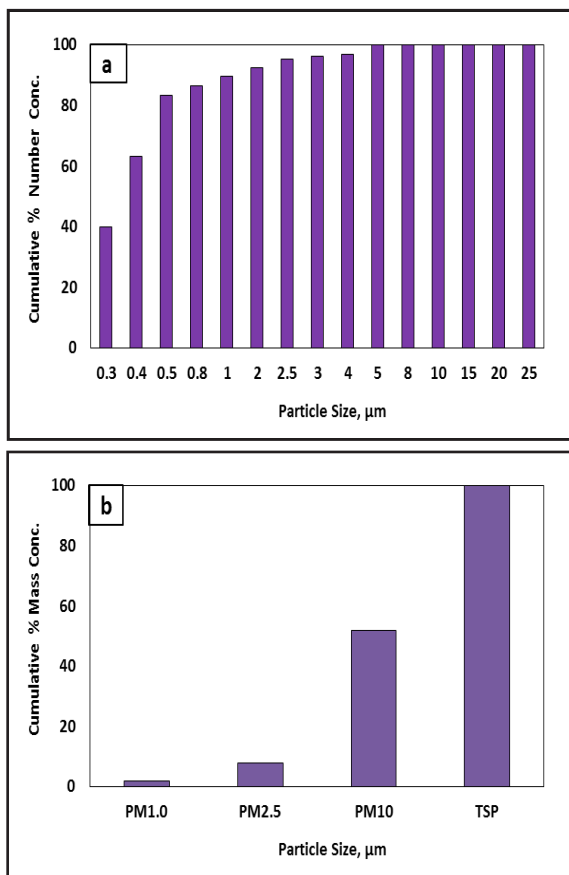


Figure 11: Measured cumulative percentage of particle size distributions, based on (a) number and (b) mass concentrations

## CONCLUSIONS

Elevated dust concentrations and dust storms associated with dustfall in the Al-Ahsa oasis region of Saudi Arabia are common phenomena that can have many adverse

effects. These can be classified as follows: effects on human and animal respiratory systems, increased indoor dust associated with animal husbandry, and adverse dust effects on plant health and productivity.

This study provides basic knowledge about the nature and characteristics of a severe dust storm struck the arid region of Al-Ahsa on 12–13 March 2014. This storm resulted in widespread and heavy dust deposition and poor visibility. During the storm, air temperature dropped by  $\sim 9\ ^\circ\text{C}$  to a maximum  $27\ ^\circ\text{C}$ , compared with an average monthly mean maximum of  $36\ ^\circ\text{C}$ . Atmospheric pressure dropped to a minimum of  $984.34\ \text{mbar}$ , in contrast with  $993.6\ \text{mbar}$  recorded the day before. Wind rapidly increased to a maximum speed of  $17.5\ \text{m/s}$  and shifted to a northerly direction, causing a dramatic decrease in visibility to  $200\ \text{m}$  with dust storm arrival. Average recorded concentrations for TSP,  $\text{PM}_{10}$  and  $\text{PM}_{2.5}$  were  $6,772$ ,  $5,862.4$  and  $451.1\ \mu\text{g}/\text{m}^3$ , respectively.

Particle size distributions revealed that GMD was  $13.58\ \mu\text{m}$ , based on mass particle concentration. However, GMD based on numerical particle concentration was  $0.48\ \mu\text{m}$ . The cumulative particle mass concentration percentage, demonstrating that the majority of particles were larger than  $2.5\ \mu\text{m}$  ( $> 85\%$ ). This study examined one dust event and one location. Therefore, more sampling periods at different locations are needed to clarify the long-term spatiotemporal effects of dust storms. More studies are also needed to link ambient and atmospheric dust effects to animal welfare and husbandry and methods of protection. Moreover, understanding of links between atmospheric dust and plant health and productivity is required. The economic impact and health effects of elevated dust concentrations and associated dustfall on residential and industrial areas is also a fertile area for future study.

## ACKNOWLEDGEMENTS

The author would like to thank the Deanship of Scientific Research of King Faisal University, Hofuf, Saudi Arabia, for financial support

(Grant No. 140038). Acknowledgements are also extended to the agencies, publishers and authors mentioned for their supportive and valuable information.

## REFERENCES

- Abdulmalik, A., Alghamdi, A. and Al-Kahtan, N. S. 2005. Sand control measures and sand drift fences. *Journal of performance of constructed facilities* ©ASCE/ November. 299.
- Ackerman, S. A. and Cox, S.K. 1989. Surface weather observations of atmospheric dust over the southwest summer monsoon region. *Meteorology and Atmospheric Physics* 41: 19–34.
- Al-Dabbas, M. A., Abbas, M.A. and Al-Khafaji, R. M. 2012. Dust storms loads analyses—Iraq. *Arab J Geosci.* 5: 121–131.
- Almuhanha, E. A., Maghirang, R. G., Murphy, J. P. and Erickson, L. E. 2009. Laboratory scale electrostatically assisted wet scrubber for controlling dust in livestock buildings. *Applied Engineering in Agriculture of the ASABE.* 25(5): 745-750.
- Almuhanha, E. A., Maghirang, R. G., Murphy, J. P. and Erickson, L. E. 2008. Effectiveness of electrostatically charged water spray in reducing dust concentration in enclosed spaces. *Transactions of the ASABE.* 51(1): 279-286.
- AL-Saud, M. 2004. Discrimination of the land features in AL Hasa Oasis, Saudi Arabia, using ratio technique on Landsat 5 ETM data. *Egyptian Journal for Remote Sensing & Space Sciences.* 4: 167-178.
- Batjargal, Z., Dulam, J. and Chung, Y. S. 2006. Dust storms are an indication of an unhealthy environment in East Asia. *Environmental Monitoring and Assessment* 114: 447–460.
- Chung, Y. S., Kim, H.S., Han K.Y. and Jugder, D. 2003. On East Asian sand and duststorms and associated significant dustfall observed from January to May 2001. *Water, Air, and Soil Pollution: Focus.* 3: 259–277.
- Gunawardena, J., Ziyath, A.M., Bostrom, T.E., Bekessy, L. K., Ayoko, G. A., Egodawatta, P. and Goonetilleke, A. 2013. Characterisation of atmospheric deposited particles during a dust storm in urban areas of Eastern Australia. *Science of the Total Environment*, 461-462: 72-80.
- Frolova, N. S., Zinchenko, G.S. and Papina, T.S. 2007. Influence of regional atmospheric processes on the formation of dust pollution layers in Belukha glacial deposits. *Russian Meteorology and Hydrology.* 32(3): 212–216.
- Fryrear, D. W. 1990. Wind Erosion: Mechanics, prediction, and control. *Adv. in Soil Sci.*, 13,187–199.
- Hassan, S. K. M. 2006. Atmospheric polycyclic aromatic hydrocarbons and some heavy metals in suspended particulate matter in urban, industrial and residential areas in greater Cairo. Ph. D. Thesis, Chemistry Department, Faculty of Science, Cairo University, Egypt.
- Hinds, W. C. 1999. *Aerosol Technology.* New York, N. Y.: John Wiley and Sons.
- Maghrabi, A., Alharbi, B. and Tapper, N. 2011. Impact of the March 2009 dust event in Saudi Arabia on aerosol optical properties, meteorological parameters, sky temperature and emissivity. *Atmospheric Environment.* 45: 2164-2173.
- Mohalfi, S. M. 1995. Sensitivity of diurnal change and synoptic features to dust aerosols over the region of Saudi Arabia. Dissertation, Florida State University. NASA, 2012. Picture Source: <http://go.nasa.gov/2fntODN>.
- PSRCEWD. 2014. Prince Sultan Research Center for Environment, Water and Desert at King Saud University. [http://www.psrcewd.edu.sa/english/article\\_71.html](http://www.psrcewd.edu.sa/english/article_71.html) Retrieval Date: 30/12/2014>.
- Shao, Y. and Dong, C. H. 2006. A review on East Asian dust storm climate, modelling and monitoring. *Global and Planetary Change.* 52: 1–22.

**العواصف الترابية في واحة الأحساء بالمملكة العربية السعودية: دراسة حالة**

عماد على المهني

قسم هندسة النظم الزراعية، كلية العلوم الزراعية والأغذية، جامعة الملك فيصل  
الأحساء، المملكة العربية السعودية

استلام 18 يناير 2015م - قبول 10 أبريل 2015م

**الملخص**

تهدف هذه الدراسة إلى وصف خصائص العواصف الغبارية في البيئة القاحلة لواحة الأحساء في المملكة العربية السعودية حيث تشتمل هذه الورقة على قياسات مفصلة للعاصفة الغبارية التي حدثت خلال 12-13 مارس 2014. تسببت هذه العاصفة في انتشار كثيف للغبار وترسب كميات كبيرة من الأتربة، رافق ذلك انخفاض كبير في مدى الرؤية الأفقية أثناء العاصفة وخلال فترة الذروة التي امتدت لفترة 10 ساعات كان متوسط التركيزات المسجلة 6772 و5862.4 و451.1 ميكروغرام/م<sup>3</sup> للقيم المتوسطة للجسيمات المعلقة الكلية (TSP) والجسيمات المعلقة بقطر يساوي (أو أصغر من) 10 ميكرومتر (PM10) والجسيمات المعلقة بقطر يساوي (أو أصغر من) 2.5 ميكرومتر (PM<sub>2.5</sub>)، على التوالي. بين التوزيع القياسي للجسيمات أن القطر الهندسي للجسيمات خلال العاصفة كان 13.58 ميكرومتر، استناداً إلى كتلة الجسيمات. إضافة إلى ذلك فإن النسبة المئوية التراكمية للتركيز الشامل للجسيمات بقطر 0.3 - 25 ميكرومتر قد بينت أن قطر أغلبية الجسيمات كان أكبر من 2.5 ميكرومتر بنسبة تتجاوز 85%. أوضحت الدراسة أن تركيز الغبار الجوي أثناء العاصفة قد تجاوز كثيراً الحدود المعيارية لجودة الهواء مما قد يؤثر على الإنسان، والحيوان، والمزروعات.

**الكلمات المفتاحية:** جودة الهواء، العواصف الغبارية، مدى الرؤية، المملكة العربية السعودية.